MAJOR ARTICLE

Nef Inhibits Glucose Uptake in Adipocytes and Contributes to Insulin Resistance in Human Immunodeficiency Virus Type I Infection

Laura Cheney,[1] June C. Hou,[1] Sidonie Morrison,[1,2] Jeffrey Pessin,[1,a] and Roy T. Steigbigel[1,2]

[1]Department of Pharmacological Sciences and [2]Department of Medicine, State University of New York at Stony Brook

Human immunodeficiency virus (HIV) infection is associated with insulin resistance. HIV type 1 Nef downregulates cell surface protein expression, alters signal transduction, and interacts with the cytoskeleton and proteins involved in actin polymerization. These functions are required for glucose uptake by insulin-stimulated adipocytes. We sought to determine whether Nef alters adipocyte glucose homeostasis. Using radiolabeled glucose, we found that adipocytes exposed to recombinant Nef took in 42% less glucose after insulin stimulation than did control cells. This reduction resulted from a Nef-dependent inhibition of glucose transporter 4 (GLUT4) trafficking, as assessed by means of immunofluorescence microscopy. Immunoblot analysis revealed a decrease in phosphorylation of signal transducing proteins after Nef treatment, and fluorescence microscopy showed a dramatic alteration in cortical actin organization. We conclude that Nef interferes with insulin-stimulated processes in adipocytes. We have identified HIV Nef, which is detectable and antigenic in serum samples from HIV-infected people, as a novel contributor to the development of insulin resistance.

Human immunodeficiency virus (HIV)-infected patients receiving antiretroviral therapy (ART) frequently develop metabolic abnormalities. These include dyslipidemia with increased risks of atherosclerosis and coronary artery disease, lipodystrophy syndromes, and failure of glucose homeostasis, including insulin resistance and Type II (non–insulin-dependent) diabetes mellitus.

The correlation between ART and metabolic abnormalities is well established, but HIV type 1 (HIV-1) drives these abnormalities as well. Alterations in blood lipid levels, lipogenesis, and triglyceride clearance were documented before the ART era [1, 2]. Giralt et al found that gene expression in primary subcutaneous adipose tissue is substantially altered, and El-Sadr et al found less evidence of insulin resistance with higher CD4 counts, but no relationship with HIV RNA level, in ART-naive HIV-1–infected patients [3, 4]. An in vitro HIV-1 infection model of T cells showed that protein expression is altered along pathways involved in lipid synthesis, transport, and metabolism [5]. Bergersen et al report a trend toward insulin resistance in ART-naive HIV-infected individuals, and a recent cross-sectional study showed that HIV viral load is an independent predictor for metabolic syndrome [6]. Additional work in vitro implicates the viral accessory proteins Vpr and Nef in the development of insulin resistance, changes in cholesterol synthesis and storage, and adipogenesis [7–9].

Pancreatic β-cells release insulin in response to hyperglycemia, stimulating muscle and adipose tissue to store sugar and blocking the liver from releasing glucose into circulation. Insulin resistance occurs when glucose uptake is insufficiently stimulated and hepatic glucose release is permitted. Persistent hyperglycemia results,

Received 21 June 2010; accepted 24 January 2011.

Potential conflicts of interest: none reported.

Presented in part: 16th Annual Conference on Retroviruses and Opportunistic Infections, Montreal, Canada, 8–11 February 2009. Abstract 720.

[a]Present address: Department of Medicine and Molecular Pharmacology , Albert Einstein College of Medicine, Bronx, New York.

Correspondence: Roy T. Steigbigel, MD, HSC T15 080, Stony Brook, NY 11794-8153 (roy.steigbigel@stonybrook.edu).

The Journal of Infectious Diseases 2011;203:1824–31

0022-1899 (print)/1537-6613 (online)/2011/20312-0017$14.00

DOI: 10.1093/infdis/jir170

with the eventual development of Type II diabetes mellitus. The estimated incidence of glucose metabolism disorders in the HIV-infected population is between 2% and 25% [10], with a 2.2-fold increase in the relative risk of Type II diabetes mellitus [11]. An earlier report, however, described an increased rate of insulin clearance and sensitivity in a small group of HIV-infected men [12]. Although HIV clearly affects lipid metabolism, its effects on glucose homeostasis, independent of ART, remain unresolved.

HIV-1 Nef is a 27 kDa nonstructural protein essential for HIV replication and propagation that also has a role in the virus's evasion of host immune responses. It contributes substantially to HIV pathogenesis [13, 14]. Nef has no known enzymatic activity but modulates a variety of cell processes through protein-protein interactions. It downregulates the cell surface expression of several proteins, including CD4 and major histocompatibility complex class I (MHCI) molecules [15–18]. It also alters signal transduction pathways [19–28] and interacts with components of the actin cytoskeleton and proteins involved in actin polymerization [29–33]. Each of these cell processes is essential for adipocyte function with regard to insulin action and glucose homeostasis. Nef is secreted into the extracellular environment and can influence cell function even in cells not competent for HIV-1 infection [20, 27, 31, 34–37]. Taken together, we hypothesized that HIV-1, via Nef, alters adipocyte function so that glucose homeostasis is perturbed.

Methods

Cell Culture Conditions

3T3L1 pre-adipocytes (ATCC) were cultured in Dulbecco's Modified Eagle's medium (DMEM) containing 25 mM glucose and 10% bovine calf serum at 37°C with 5% CO_2. Two days past confluence, cells were differentiated into adipocytes with DMEM containing 10% fetal bovine serum (FBS), 1 μg/mL insulin (Sigma-Aldrich), 1 μM dexamethasone (Sigma-Aldrich), and 0.5 mM isobutyl-1-methylxanthine (Sigma-Aldrich). Media were replaced with DMEM containing 10% FBS and 1 μg/mL insulin on the fourth day of differentiation. Before experiments, cells were treated overnight with 0.1 μg/mL recombinant myristoylated HIV-1 Nef (Jena Biosciences) or nonmyristoylated Nef (National Institutes of Health AIDS Reference and Reagent Repository) unless noted otherwise. Cells were serum-starved in DMEM for 2–3 h before continuing.

Glucose Uptake Assay

Adipocytes were inoculated onto 24-well culture plates and treated overnight with 0.005, 0.01, 0.05, and 0.1 μg/mL recombinant myristoylated HIV-1 Nef. Cells were serum-starved, washed twice with Krebs–Ringer bicarbonate buffer containing 30 mM HEPES, pH 7.4, and 0.1% bovine seroalbumin (BSA) (Krebs–Ringer bicarbonate/HEPES [KRBH]/BSA) and incubated in KRBH/BSA for 30 min. Two wells per treatment were incubated in KRBH/BSA/0.4 mM Cytochalasin B (Sigma-Aldrich) to determine nonspecific glucose uptake. Cells were left unstimulated or stimulated with 10 nM insulin for 20 min. The assay was initiated by addition of 2-deoxyglucose-D-[1-^{3}H] glucose (1 μCi per well; Amersham Biosciences) and 0.1 mM 2-deoxyglucose. The assay was terminated after 10 min with phosphate-buffered saline (PBS) containing 10 mM glucose and 0.2 mM Cytochalasin B. Cells were washed 3 times with ice-cold PBS/10 mM glucose. Cell lysates were collected in 0.05 N NaOH/1% Triton X-100. Protein concentrations were determined by means of BCA protein assay (Pierce). Cell-associated radioactivity (disintegrations per minute) was normalized to the protein concentration.

Transient GLUT4 Transfection and Immunofluorescence Studies

Adipocytes were transfected with a Myc-GLUT4–green fluorescent protein (GFP) construct described elsewhere [38] with Gene Pulser II (Bio-Rad) using 0.16 kV and 950 μF. Following electroporation, cells were inoculated onto glass coverslips and allowed to recover for 12–16 h. Cells were treated with Nef as described, then stimulated with either 10 or 100 nM insulin for 20 min or left unstimulated. Adipocytes were fixed for 10 min in 4% paraformaldehyde and blocked in 5% donkey serum (Sigma-Aldrich) containing 1% BSA (Sigma-Aldrich) for 1 h at room temperature. Cells were probed with c-Myc 9E10 monoclonal antibody (Santa Cruz Biotechnology) and stained with Texas-Red conjugated donkey anti-mouse IgG antibody (Jackson Immunoresearch Laboratories) prior to mounting with Vectashield (Vector Labs). Fluorescence images were acquired by confocal fluorescence microscopy, and fluorescence intensity measurements were performed using Zeiss LSM510 software. The degree of GLUT4 *fusion* with the plasma membrane was quantified by measuring Texas Red fluorescence at the plasma membrane and normalizing to the GFP signal of the whole cell. The degree of GLUT4 *translocation* to the plasma membrane was quantified similarly: GFP signal at the plasma membrane was normalized to total GFP signal of the cell. Twenty-five cells were analyzed per condition.

Actin Polymerization Assay

Adipocytes were inoculated onto coverslips and treated as described, except for 1 group in which 20 μM Latrunculin B (LatB; Sigma-Aldrich) was added during serum starvation. Cells were stimulated with 10 nM insulin for 20 min. Cells were fixed as above and stained with rhodamine-conjugated phalloidin (Invitrogen). Coverslips were mounted on glass slides with Vectashield containing 4′,6-diamidino-2-phenylindole (Vector Labs). Fluorescent images were obtained as above. Fifty rhodamine-stained cells per condition were scored positive or negative on the basis of the morphology of the circumferential filamentous (F)-actin ring. Cells with discontinuous fluorescence rims were

scored positive, whereas cells with smooth rims were scored negative.

Immunoblotting

Adipocytes were stimulated with 0, 10, or 100 nM insulin for 7 min. Cells were washed with PBS and collected in radioimmunoprecipitation assay buffer containing Protease Inhibitor Cocktail and Phosphatase Inhibitor Cocktail 3 (Sigma-Aldrich). After rotation at 4° for 10 min, lysates were clarified at 15,000 rpm for 15 min at 4°C. Protein concentrations were quantified by BCA protein assay. Equal amounts of protein from each sample were resolved by sodium dodecyl sulfate–polyacrylamide gel electrophoresis. Gels were immunoblotted with monoclonal phospho-Akt (Ser-473) antibody (Cell Signal Technology), polyclonal phospho-AS160 (Thr-642) antibody (Millipore), polyclonal phospho–neural Wiskott-Aldrich syndrome protein (N-WASP) (Tyr-256) antibody (ECM Biosciences), or polyclonal phospho–N-WASP (Ser 484/485) antibody where indicated and visualized with SuperSignal West chemiluminescent substrate (Pierce). Membranes were stripped and reprobed with polyclonal rabbit antibodies to total Akt (Cell Signaling Technology), total AS-160 (Millipore), or total N-WASP (ECM Biosciences), where indicated. Semiquantitative analysis was performed using ImageJ software (National Institute of Health). The optical density of the phosphorylated protein was divided by the optical density of the total protein minus background.

Data Analysis

Experiments were independently performed $\geq$ 3 times. Significance values of all experiments were calculated by means of a 2-tailed paired-samples *t* test using SPSS version 12.0.

RESULTS

Nef Inhibits Insulin-Stimulated Glucose Uptake in 3T3L1 Cultured Adipocytes

Insulin-stimulated glucose uptake in skeletal muscle and adipocytes is required for maintaining postprandial blood glucose homeostasis. We measured glucose uptake in response to 10 nM insulin in differentiated 3T3L1 adipocytes treated with HIV Nef. In the absence of insulin stimulation, there was no difference in the mean basal glucose uptake between control and myristoylated Nef–treated cells at any Nef concentration (Figure 1A), indicating that exposure to Nef did not affect basal metabolic processes. Upon stimulation with 10 nM insulin, control adipocytes displayed an approximate 5-fold increase in glucose uptake after insulin stimulation, compared with unstimulated cells (Figure 1A and B). In contrast, Nef treatment significantly reduced the mean rate of insulin-stimulated glucose uptake in a dose-dependent manner, compared with control cells. Glucose uptake was reduced by 42% in cells treated with 0.1 μg/mL Nef

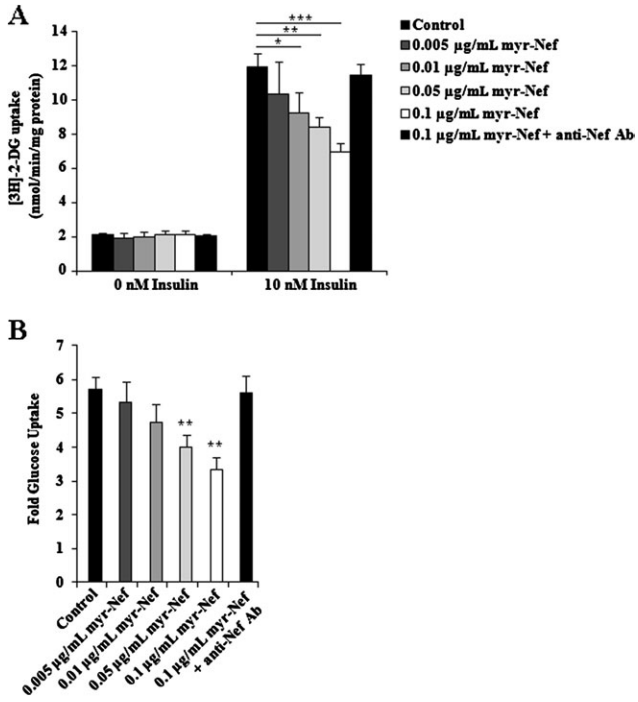

Figure 1. Glucose uptake by control and myristoylated Nef (myr-Nef)–treated adipocytes expressed as (*A*) the mean rate of [^{3}H]-2-deoxyglucose (2-DG) uptake and (*B*) the fold glucose uptake over basal uptake. Values represent the mean ± standard deviation of triplicate determinations. Asterisk, $P < .05$; double asterisk, $P < .02$; triple asterisk, $P < .005$.

($P = .005$), by 29% with 0.05 μg/mL Nef ($P = .016$), and by 22% with 0.01 μg/mL Nef ($P = .028$) relative to control cells (Figure 1A and B). Treatment with 0.005 μg/mL Nef also reduced glucose uptake relative to control cells by approximately 13%, although statistical significance was not achieved (Figure 1A and B). There was also no difference in the mean basal glucose uptake between control cells and cells treated with 0.1 μg/mL nonmyristoylated Nef ($P = .16$), whereas the mean rate of glucose uptake by nonmyristoylated Nef–treated cells stimulated with 10 nM insulin was significantly reduced ($P = .014$). Thus, Nef treatment resulted in a significant dose-dependent reduction of insulin-stimulated glucose uptake.

To ensure Nef specificity, cells were also treated overnight with a mixture of 0.1 μg/mL Nef plus excess polyclonal anti-HIV Nef antibody. There was no significant difference in glucose uptake between control and Nef/anti-Nef–treated adipocytes (Figure 1A, $P = .07$; Figure 1B, $P = .72$). Exposure to Nef did not affect the viability of the adipocytes, because the proportions of viable control cells and Nef-treated cells were the same (80%) as determined by Trypan Blue exclusion.

Nef Inhibits GLUT4 Fusion With the Plasma Membrane in Insulin-Stimulated Adipocytes

GLUT4 is the primary insulin-responsive glucose transporter in adipocytes. In unstimulated cells, GLUT4 accumulates in intracellular compartments but is rapidly translocated to the

plasma membrane upon insulin stimulation. Subsequent integration with the plasma membrane allows for glucose influx. Since Nef is associated with alterations in cell surface protein expression, we sought to determine whether the decrease in glucose uptake by Nef-treated cells was due to a decrease in GLUT4 surface expression. Differentiated adipocytes were transiently transfected with a Myc-GLUT4-GFP plasmid and stimulated with insulin as described above. Staining the exofacial myc tag of unpermeabilized cells permits sensitive and quantitative measurements of the amount of GLUT4 integration into the plasma membrane after insulin stimulation. Little or no GLUT4 was inserted into the plasma membranes of unstimulated control cells or cells exposed to 0.1 μg/mL myristoylated Nef, as evidenced by the lack of red fluorescence at the plasma membrane (Figure 2A, left and right panels, respectively). There was no significant difference in the mean red fluorescence intensity between unstimulated control and Nef-treated cells (Figure 2B; $P = .09$).

After stimulation of control adipocytes with 10 or 100 nM insulin, there was dose-responsive integration of GLUT4 with the plasma membrane (Figure 2C, panels 1 and 7). In contrast, adipocytes treated with 0.1 μg/mL Nef appeared markedly different from control cells stimulated with the same insulin concentrations. GLUT4 integration into the plasma membranes of Nef-treated cells was substantially less and appeared punctate (Figure 2C, panel 4 vs 1 and panel 10 vs 7). Accordingly, there was a significant reduction in the mean fluorescence intensity at the plasma membranes of Nef-treated, insulin-stimulated cells. After 10 nM insulin stimulation, Nef-treated cells displayed an approximately 31% reduction relative to control cells (Figure 2B, $P = .045$), and after 100 nM insulin, they displayed an approximately 36% reduction relative to control cells (Figure 2B, $P = .029$). These data indicate that Nef inhibits insulin-induced GLUT4 fusion with the plasma membrane.

Nonmyristoylated Nef also decreased insulin-stimulated GLUT4 fusion relative to control cells. With no insulin stimulation, there was no significant reduction in the mean fluorescence intensity at the plasma membranes of Nef-treated cells, compared with control cells, but there was a significant decrease after stimulation with 10 nM insulin ($P = .046$) and after stimulation with 100 nM insulin ($P = .029$). Treatment with nonmyristoylated Nef decreased fluorescence intensity by 32% relative to control cells after 10 nM insulin stimulation and by 64% relative to control cells after 100 nM insulin stimulation.

Because Nef was added directly to adipocyte culture media, we wanted to ensure that Nef did not interfere with binding of the myc antibody to its epitope, generating a false reduction in fluorescence intensity. To address this, stimulated control cells were probed with a mixture of the myc antibody and 0.1 μg/mL Nef. There was no significant difference in the fluorescence intensity between control cells and cells probed with the myc antibody/Nef mixture ($P = .27$), indicating that exogenous Nef did not interfere with antibody recognition of the myc epitope.

A decrease in the insertion of GLUT4 into the plasma membrane when Nef is present may be due to a decrease in the amount of GLUT4 translocated to the plasma membrane from

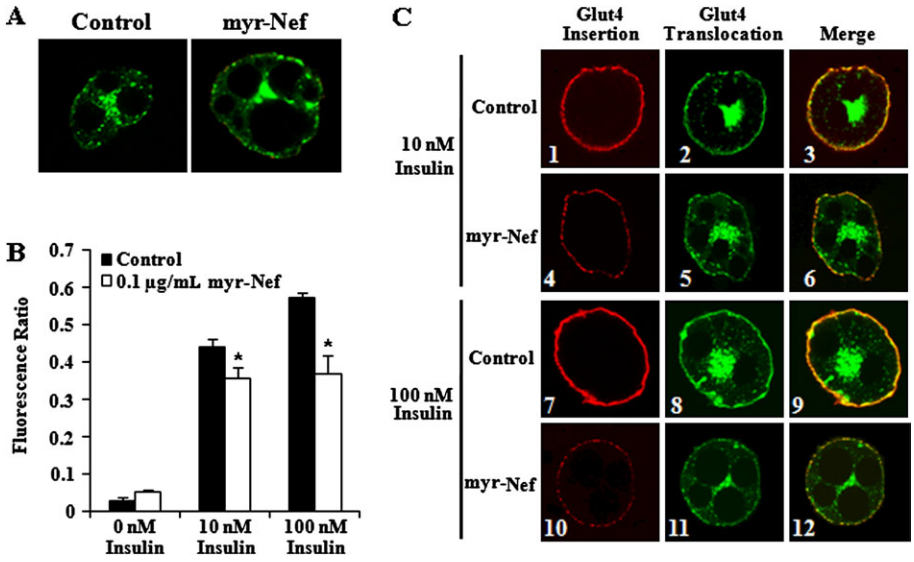

Figure 2. Glucose transporter 4 (GLUT4) fusion and translocation in insulin-stimulated control and myristoylated Nef–treated adipocytes. *A,C,* Immunofluorescence analysis of Myc–GLUT4–green fluorescence protein (GFP)–transfected control and Nef-treated adipocytes with no insulin stimulation (*A*), and 10 or 100 nM insulin stimulation (*C*), stained with mouse monoclonal antibody to c-Myc followed by Texas Red–conjugated rabbit anti–mouse IgG. Original magnification, ×63. *C,* The yellow fluorescence in panels 3, 6, 9, and 12 confirms that the red and green fluorescence represents the same, insulin-responsive protein. (*B*) The red fluorescence intensity of Myc-GLUT4-GFP transfected control and Nef-treated cells with no insulin or 10 or 100 nM insulin stimulation. Values represent the mean ± standard deviation of 3 independent experiments. $^*P < .05$.

intracellular storage sites after insulin stimulation. The GFP tag on the GLUT4 molecule was utilized to quantify GLUT4 translocation after insulin stimulation. As expected, there was little GLUT4 translocation to the plasma membrane without insulin stimulation, with most GLUT4 occupying a perinuclear space (Figure 2A, left panel). Unstimulated Nef-exposed adipocytes appeared similar with little to no translocation (Figure 2A, right panel). There was no significant difference in the mean green fluorescence intensity between control and Nef-treated cells without insulin stimulation ($P = .44$). After 10 nM insulin stimulation, there was a difference in the degree of GLUT4 translocation between control and Nef-treated cells (Figure 2C, panels 2 and 5, respectively) and also a difference between control and Nef-treated cells after 100 nM insulin stimulation (Figure 2C, panels 8 and 11, respectively). The yellow fluorescence in panels 3, 6, 9, and 12 of Figure 2C confirms that the red and green fluorescence represents the same, insulin-responsive protein. Quantitative analysis confirmed a significant difference in mean green fluorescence intensity between Nef-treated and control cells after 10 nM insulin stimulation ($P = .004$) and after 100 nM insulin stimulation ($P = .009$). These data suggest that Nef affects the trafficking of GLUT4 to the plasma membrane.

Nef Alters the Proximal Signal Transduction Pathway of Insulin

Activation of Akt via phosphorylation is required for insulin-stimulated GLUT4 mobilization [39]. To determine whether the decrease in GLUT4 trafficking observed in Nef-treated cells was due to disruption of the proximal insulin signal transduction cascade, we performed immunoblot analysis of Akt phosphorylation. Without insulin stimulation, cell lysates revealed minimal phosphorylation of Akt in either control or Nef-treated cells (Figure 3A). The degree of phosphorylation increased dose-dependently with insulin concentration in control cells. However, there was considerably less Akt phosphorylation in Nef-treated lysates relative to control lysates at either 10 nM insulin (11% of control Akt phosphorylation) and 100 nM insulin (32% of control Akt phosphorylation) (Figure 3B).

To substantiate the downstream consequences of this proximal effect of Nef, we analyzed the phosphorylation of AS160. Phosphorylation patterns of AS160 in Nef-treated, insulin-stimulated adipocytes were similar to those of Akt, with considerably less phosphorylation relative to control lysates at either insulin concentration (Figure 3A and B). These data indicate that Nef influences insulin-stimulated signaling cascades in adipocytes.

Nef Disrupts F-Actin at the Cortical Actin Ring

Dynamic changes of adipocyte cortical actin meshwork are required for GLUT4 translocation and fusion with the plasma membrane [40, 41]. To determine whether the decrease in GLUT4 fusion in cells treated with nonmyristoylated Nef was attributable to disruption of actin polymerization dynamics, we examined actin organization in control, Nef-treated, and LatB-

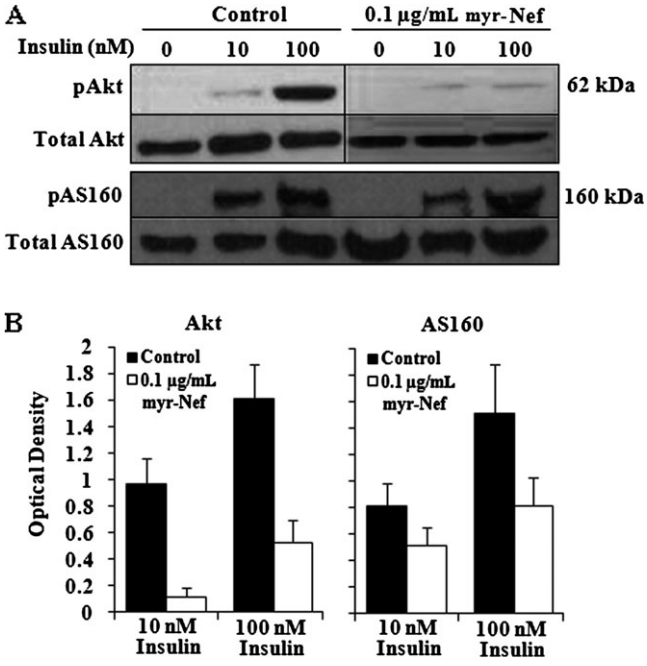

Figure 3. Akt and AS160 phosphorylation in control and myristoylated Nef–treated adipocytes stimulated with 10 or 100 nM insulin. *A,* Immunoblot of Akt and AS160 phosphorylation. *B,* Quantitation of immunoblots for Akt and AS160 phosphorylation. Values shown are, respectively, the average ratio ± standard deviation of phospho-Akt or phospho-AS160 to total Akt or total AS160, expressed as optical density minus background from at least 2 independent immunoblots.

treated cells. As expected, control cells had very smooth, intact cortical actin without and with 10 nM insulin stimulation (Figure 4A, panels 1 and 4, respectively), while LatB-treated cells revealed substantial cortical actin perturbations (Figure 4A, panels 3 and 6, respectively). Nef-treated cells were morphologically intermediate, with perturbation of the actin rings under basal and insulin-stimulated conditions, although not to the degree seen in LatB-treated cells (Figure 4A, panels 2 and 5, respectively). This qualitative assessment was confirmed quantitatively as described above. Only a small number of control cells were positive for disrupted F-actin (8.7%; Figure 4B), whereas a high proportion of LatB-treated cells had disrupted cortical actin polymers (89.3%; Figure 4B). Nef-treated cells had a result between those of control and LatB-treated cells, with 56.7% showing perturbed cortical F-actin (Figure 4B). Compared with control cells, there was a significant difference in the proportion of Nef-treated cells with disrupted cortical actin, both unstimulated and stimulated ($P = .019$ and .047, respectively). These data indicate that actin dynamics are disrupted in adipocytes exposed to Nef.

Insulin induces cortical ring localization of N-WASP, a requirement for actin filament rearrangement in adipocytes [42]. N-WASP phosphorylation stabilizes the "open" confirmation, enhancing its activity toward the Arp2/3 complex. We performed immunoblot analysis of N-WASP phosphorylation to

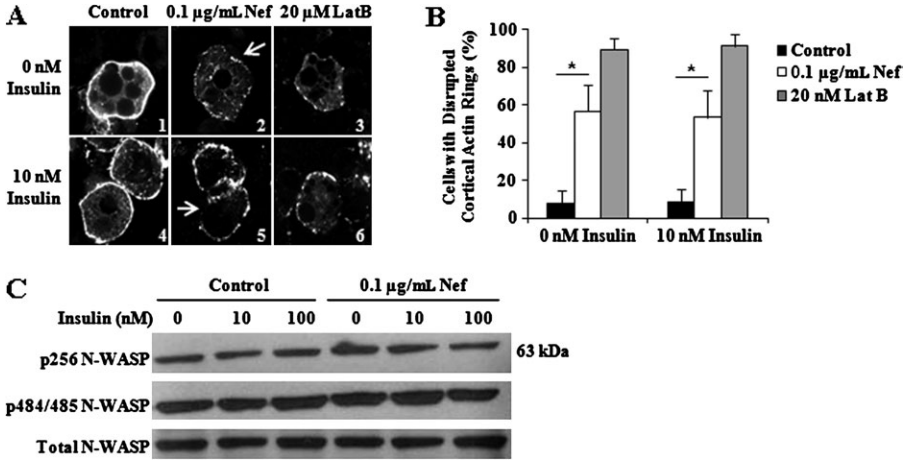

Figure 4. Cortical actin rings of control, Nef-treated, and Latrunculin B–treated adipocytes. *A,* Fluorescence microscopy of control, Nef-treated, and Latrunculin B–treated adipocytes without and with 10 nM insulin stimulation. Cells were stained with rhodamine-conjugated phalloidin. The arrows (panels 2 and 5) designate areas of disrupted F-actin. *B,* The percent of control, Nef-treated, and Latrunculin B–treated cells with perturbed cortical actin, without and with 10 nM insulin stimulation. Values are the mean percent of cells positive for disrupted actin ± the standard deviation from 3 independent experiments. $*P < .05$. *C,* Neural Wiskott-Aldrich syndrome protein (N-WASP) phosphorylation in control and Nef-treated adipocytes unstimulated or stimulated with 10 or 100 nM insulin.

determine whether the cortical actin perturbations caused by Nef were due to alterations in N-WASP phosphorylation. There was no difference between control and nonmyristoylated Nef-treated cells in the degree of phosphorylation at Tyr-256 whether stimulated with 10 or 100 nM insulin or not (Figure 4C). N-WASP is constitutively phosphorylated at Ser-484 and Ser-485. We detected no difference between control and Nef-exposed adipocytes in phosphorylation rates at these residues (Figure 4C).

DISCUSSION

Although there are important links between ART and insulin resistance in HIV infection, HIV also causes metabolic disturbances directly. We provide new insights into how HIV-1 affects adipocyte function in glucose homeostasis. We show that HIV-1 Nef significantly reduces glucose uptake in insulin-stimulated adipocytes by inhibiting GLUT4 surface expression. Nef also inhibits insulin-induced signal transduction and cortical actin dynamics prohibiting GLUT4 translocation and fusion with the plasma membrane.

Pancreatic β-cells release insulin when the blood level of glucose increases. Insulin binds its receptor on adipocytes, inducing events that culminate in glucose uptake. Vesicles containing GLUT4 are mobilized from the insulin-responsive compartment and translocated to the plasma membrane where fusion initiates glucose influx. We found that after exposure to Nef, insulin-stimulated adipocytes took in less glucose than control adipocytes in a dose-dependent manner (Figure 1). This effect was Nef-specific, as glucose uptake by cells treated simultaneously with Nef and anti-Nef antibody was similar to that of control cells. Nef caused no detectable cytotoxicity, as basal glucose uptake and viability were similar between control and Nef-treated cells.

Decreased glucose uptake is attributable to a Nef-dependent reduction in surface expression of GLUT4 molecules (Figure 2B), a finding consistent with the known ability of exogenous Nef to change expression of cell surface proteins [36, 37]. The mechanism by which Nef inhibits GLUT4 translocation and fusion after stimulation is not fully understood. Our data suggest that Nef affects multiple cell processes. First, insulin activates a number of signaling cascades, some involving Akt. In Nef-exposed adipocytes stimulated with insulin, phosphorylation of Akt and its effector AS160 was considerably less than in control cells (Figure 3). That Nef alters signal transduction in our model is consistent with published reports that signal transduction changes in the presence of exogenous Nef [23, 24, 26, 34]. Thus, Nef-induced inhibition of GLUT4 translocation likely occurs because Akt and AS-160 are inadequately activated. Second, insulin-stimulated rearrangements within the cortical actin meshwork induce docked GLUT4 vesicles to fuse with the plasma membrane [40]. Nef disrupts actin-remodeling processes and alters cytoskeletal structure [29–33]. Our data are consistent with these published reports, as atypical cortical actin was noted in Nef-treated adipocytes (Figure 4). Although N-WASP phosphorylation is decreased in T cells expressing Nef [30], it was not decreased in the adipocytes that we studied (Figure 4C). This suggests that the cortical actin ring defect is not due to decreased N-WASP activity per se. Hence, the mechanism by which Nef alters adipocyte cortical actin rings remains undefined. These results cannot rule out the possibility that Nef interferes with secretory

trafficking proteins analogously to CD4 and MHCI molecules [15–18]. Nef likely acts at several points along the insulin-stimulated GLUT4 trafficking pathway, which would be consistent with its ability to bind a plethora of proteins and influence numerous cellular processes.

Native Nef is cotranslationally myristoylated, a modification critical to many Nef activities. However, myristoylation is not an absolute requirement. Several reports document attenuation, rather than abolition, of Nef activity, and others report Nef activities occurring without myristoylation [34, 43–46]. Because the Nef in certain experiments described here was non-myristoylated, our measurements may underestimate the degree to which native Nef alters adipocyte function.

Nef lacks the canonical secretory signal sequence, yet is released extracellularly and is detectable in the serum samples of HIV-infected people in amounts up to 50 ng/mL ([27]; L. Cheney, unpublished data). There is increasing evidence that exogenous Nef induces signaling effects in cell culture [19–28]. Recombinant Nef also accumulates within primary human monocyte-derived macrophages, B cells, and dendritic cells in vitro, and native Nef is detected in uninfected primary lymphoid B cells ex vivo [20, 31, 34, 36, 37]. Adipocytes can support viral entry, as they do express all the necessary HIV receptors, and replication can occur at least to a small degree in adipocytes [47]. Therefore, it seems likely that adipocytes are exposed to Nef, although it remains unknown whether Nef acts on adipocytes in an intra- or extracellular manner, or both. Nevertheless, we hypothesize that adipocytes that are chronically exposed to Nef in vivo, as modeled in the experiments described, are impaired sufficiently to lower the threshold for development of insulin resistance in HIV-infected individuals.

Our findings implicate Nef in the development of HIV-associated insulin resistance and Type II diabetes mellitus, an important finding in light of the prolonged life expectancy that ART affords HIV-infected individuals. The HIV-infected population will be subject to the same forces that drive insulin resistance in the general population as it ages, with the added risks of HIV-associated factors, such as Nef. Further exploration of the role that HIV plays in the development of insulin resistance is vital for enhancing the clinical management of HIV disease.

Funding

This work was supported by National Institutes of Health (NIH) Medical Scientist Training Program (MSTP) grant GM00855 (to L. C.) and a Pharmaceutical Research and Manufacturers of America (PhRMA) Foundation pre-doctoral Fellowship (to L. C.). Additional support was provided by grants DK033823, DK020541, and 5-MO1-RR-10710 from the NIH.

Acknowledgments

The following reagent was obtained through the NIH AIDS Research and Reference Reagent Program, Division of AIDS, NIAID, NIH: HIV-1 Nef Protein (Cat# 11478). We thank Mark O'Hara, PhD, for his contribution to the actin polymerization assays, Dumaine Williams, PhD, Nicola Kreglinger, and Yan Tang for help with adipocyte culture, and Robert Watson, PhD, for his assistance with fluorescence microscopy and thoughtful discussions about the manuscript.

References

1. Grunfeld C, Pang M, Doerrler W, Shigenaga JK, Jensen P, Feingold KR. Lipids, lipoproteins, triglyceride clearance, and cytokines in human immunodeficiency virus infection and the acquired immunodeficiency syndrome. J Clin Endocrinol Metab **1992**; 74:1045–52.
2. Hellerstein MK, Grunfeld C, Wu K, et al. Increased de novo hepatic lipogenesis in human immunodeficiency virus infection. J Clin Endocrinol Metab **1993**; 76:559–65.
3. El-Sadr WM, Mullin CM, Carr A, et al. Effects of HIV disease on lipid, glucose and insulin levels: results from a large antiretroviral-naive cohort. HIV Med **2005**; 6:114–21.
4. Giralt M, Domingo P, Guallar JP, et al. HIV-1 infection alters gene expression in adipose tissue, which contributes to HIV-1/HAART-associated lipodystrophy. Antivir Ther **2006**; 11:729–40.
5. Rasheed S, Yan JS, Lau A, Chan AS. HIV replication enhances production of free fatty acids, low density lipoproteins and many key proteins involved in lipid metabolism: a proteomics study. PLoS One **2008**; 3:e3003.
6. Squillace N, Zona S, Stentarelli C, et al. Detectable HIV viral load is associated with metabolic syndrome. J Acquir Immune Defic Syndr **2009**; 52:459–64.
7. Kino T, De Martino MU, Charmandari E, Ichijo T, Outas T, Chrousos GP. HIV-1 accessory protein Vpr inhibits the effect of insulin on the Foxo subfamily of forkhead transcription factors by interfering with their binding to 14-3-3 proteins: potential clinical implications regarding the insulin resistance of HIV-1-infected patients. Diabetes **2005**; 54:23–31.
8. van 't Wout AB, Swain JV, Schindler M, et al. Nef induces multiple genes involved in cholesterol synthesis and uptake in human immunodeficiency virus type 1-infected T cells. J Virol **2005**; 79:10053–8.
9. Otake K, Omoto S, Yamamoto T, et al. HIV-1 Nef protein in the nucleus influences adipogenesis as well as viral transcription through the peroxisome proliferator-activated receptors. AIDS **2004**; 18:189–98.
10. Samaras K. Prevalence and pathogenesis of diabetes mellitus in HIV-1 infection treated with combined antiretroviral therapy. J Acquir Immune Defic Syndr **2009**; 50:499–505.
11. Brown TT, Cole SR, Li X, et al. Antiretroviral therapy and the prevalence and incidence of diabetes mellitus in the multicenter AIDS cohort study. Arch Intern Med **2005**; 165:1179–84.
12. Hommes MJ, Romijn JA, Endert E, Eeftinck Schattenkerk JK, Sauerwein HP. Insulin sensitivity and insulin clearance in human immunodeficiency virus-infected men. Metabolism **1991**; 40:651–6.
13. Kestler HW 3rd, Ringler DJ, Mori K, et al. Importance of the Nef gene for maintenance of high virus loads and for development of AIDS. Cell **1991**; 65:651–62.
14. Sugimoto C, Tadakuma K, Otani I, et al. Nef gene is required for robust productive infection by simian immunodeficiency virus of T-cell-rich paracortex in lymph nodes. J Virol **2003**; 77:4169–80.
15. Burtey A, Rappoport JZ, Bouchet J, et al. Dynamic interaction of HIV-1 Nef with the clathrin-mediated endocytic pathway at the plasma membrane. Traffic **2007**; 8:61–76.
16. Chaudhuri R, Lindwasser OW, Smith WJ, Hurley JH, Bonifacino JS. Downregulation of CD4 by human immunodeficiency virus type 1 Nef is dependent on clathrin and involves direct interaction of Nef with the AP2 clathrin adaptor. J Virol **2007**; 81:3877–90.
17. Kasper MR, Collins KL. Nef-mediated disruption of HLA-A2 transport to the cell surface in T cells. J Virol **2003**; 77:3041–9.
18. Roeth JF, Williams M, Kasper MR, Filzen TM, Collins KL. HIV-1 Nef disrupts MHC-I trafficking by recruiting AP-1 to the MHC-I cytoplasmic tail. J Cell Biol **2004**; 167:903–13.
19. Tobiume M, Fujinaga K, Suzuki S, Komoto S, Mukai T, Ikuta K. Extracellular Nef protein activates signal transduction pathway from Ras

to mitogen-activated protein kinase cascades that leads to activation of human immunodeficiency virus from latency. AIDS Res Hum Retroviruses **2002**; 18:461–7.
20. Quaranta MG, Camponeschi B, Straface E, Malorni W, Viora M. Induction of interleukin-15 production by HIV-1 Nef protein: a role in the proliferation of uninfected cells. Exp Cell Res **1999**; 250:112–21.
21. Mangino G, Percario ZA, Fiorucci G, et al. In vitro treatment of human monocytes/macrophages with myristoylated recombinant Nef of human immunodeficiency virus type 1 leads to the activation of mitogen-activated protein kinases, IkappaB kinases, and interferon regulatory factor 3 and to the release of beta interferon. J Virol **2007**; 81:2777–91.
22. James CO, Huang MB, Khan M, Garcia-Barrio M, Powell MD, Bond VC. Extracellular Nef protein targets $CD4^+$ T cells for apoptosis by interacting with CXCR4 surface receptors. J Virol **2004**; 78:3099–109.
23. Quaranta MG, Mattioli B, Spadaro F, et al. HIV-1 Nef triggers Vav-mediated signaling pathway leading to functional and morphological differentiation of dendritic cells. FASEB J **2003**; 17:2025–36.
24. Percario Z, Olivetta E, Fiorucci G, et al. Human immunodeficiency virus type 1 (HIV-1) Nef activates STAT3 in primary human monocyte/macrophages through the release of soluble factors: involvement of Nef domains interacting with the cell endocytotic machinery. J Leukoc Biol **2003**; 74:821–32.
25. Varin A, Manna SK, Quivy V, et al. Exogenous Nef protein activates NF-kappa B, AP-1, and c-Jun N-terminal kinase and stimulates HIV transcription in promonocytic cells: role in AIDS pathogenesis. J Biol Chem **2003**; 278:2219–27.
26. Federico M, Percario Z, Olivetta E, et al. HIV-1 Nef activates STAT1 in human monocytes/macrophages through the release of soluble factors. Blood **2001**; 98:2752–61.
27. Fujii Y, Otake K, Tashiro M, Adachi A. Soluble Nef antigen of HIV-1 is cytotoxic for human $CD4^+$ T cells. FEBS Lett **1996**; 393:93–6.
28. Fujinaga K, Zhong Q, Nakaya T, et al. Extracellular Nef protein regulates productive HIV-1 infection from latency. J Immunol **1995**; 155:5289–98.
29. Haller C, Rauch S, Fackler OT. HIV-1 Nef employs two distinct mechanisms to modulate Lck subcellular localization and TCR induced actin remodeling. PLoS One **2007**; 2:e1212.
30. Haller C, Rauch S, Michel N, et al. The HIV-1 pathogenicity factor Nef interferes with maturation of stimulatory T-lymphocyte contacts by modulation of N-Wasp activity. J Biol Chem **2006**; 281:19618–30.
31. Xu W, Santini PA, Sullivan JS, et al. HIV-1 evades virus-specific IgG2 and IgA responses by targeting systemic and intestinal B cells via long-range intercellular conduits. Nat Immunol **2009**; 10:1008–17.
32. Fackler OT, Luo W, Geyer M, Alberts AS, Peterlin BM. Activation of Vav by Nef induces cytoskeletal rearrangements and downstream effector functions. Mol Cell **1999**; 3:729–39.
33. Campbell EM, Nunez R, Hope TJ. Disruption of the actin cytoskeleton can complement the ability of Nef to enhance human immunodeficiency virus type 1 infectivity. J Virol **2004**; 78:5745–55.
34. Qiao X, He B, Chiu A, Knowles DM, Chadburn A, Cerutti A. Human immunodeficiency virus 1 Nef suppresses CD40-dependent immunoglobulin class switching in bystander B cells. Nat Immunol **2006**; 7:302–10.
35. Lehmann MH, Walter S, Ylisastigui L, et al. Extracellular HIV-1 Nef increases migration of monocytes. Exp Cell Res **2006**; 312:3659–68.
36. Alessandrini L, Santarcangelo AC, Olivetta E, et al. T-tropic human immunodeficiency virus (HIV) type 1 Nef protein enters human monocyte-macrophages and induces resistance to HIV replication: a possible mechanism of HIV T-tropic emergence in AIDS. J Gen Virol **2000**; 81:2905–17.
37. Quaranta MG, Tritarelli E, Giordani L, Viora M. HIV-1 Nef induces dendritic cell differentiation: a possible mechanism of uninfected $CD4^+$ T cell activation. Exp Cell Res **2002**; 275:243–54.
38. Kanzaki M, Furukawa M, Raab W, Pessin JE. Phosphatidylinositol 4,5-bisphosphate regulates adipocyte actin dynamics and GLUT4 vesicle recycling. J Biol Chem **2004**; 279:30622–33.
39. Gonzalez E, McGraw TE. Insulin signaling diverges into Akt-dependent and -independent signals to regulate the recruitment/docking and the fusion of GLUT4 vesicles to the plasma membrane. Mol Biol Cell **2006**; 17:84–4493.
40. Kanzaki M, Pessin JE. Insulin-stimulated GLUT4 translocation in adipocytes is dependent upon cortical actin remodeling. J Biol Chem **2001**; 276:42436–44.
41. Tong P, Khayat ZA, Huang C, Patel N, Ueyama A, Klip A. Insulin-induced cortical actin remodeling promotes GLUT4 insertion at muscle cell membrane ruffles. J Clin Invest **2001**; 108:371–81.
42. Jiang ZY, Chawla A, Bose A, Way M, Czech MP. A phosphatidylinositol 3-kinase-independent insulin signaling pathway to N-WASP/Arp2/3/F-actin required for GLUT4 glucose transporter recycling. J Biol Chem **2002**; 277:509–15.
43. Chowers MY, Spina CA, Kwoh TJ, Fitch NJ, Richman DD, Guatelli JC. Optimal infectivity in vitro of human immunodeficiency virus type 1 requires an intact Nef gene. J Virol **1994**; 68:2906–2914.
44. Fackler OT, Moris A, Tibroni N, et al. Functional characterization of HIV-1 Nef mutants in the context of viral infection. Virology **2006**; 351:322–39.
45. Harris M, Coates K. Identification of cellular proteins that bind to the human immunodeficiency virus type 1 Nef gene product in vitro: a role for myristylation. J Gen Virol **1993**; 74(pt 8);1581–9.
46. Briggs SD, Scholtz B, Jacque JM, Swingler S, Stevenson M, Smithgall TE. HIV-1 Nef promotes survival of myeloid cells by a Stat3-dependent pathway. J Biol Chem **2001**; 276:25605–11.
47. Hazan U, Romero IA, Cancello R, et al. Human adipose cells express CD4, CXCR4, and CCR5 [corrected] receptors: a new target cell type for the immunodeficiency virus-1? FASEB J **2002**; 16:1254–6.